INT. J. REMOTE SENSING, 1988, VOL. 9, NO. 5, 997–1011

125

SIR-B stereo-radargrammetry of Australia

F. LEBERL, W. MAYR and G. DOMIK†

VEXCEL Corporation, 2905 Wilderness Place, Boulder, Colorado 80301, U.S.A.

and M. KOBRICK

Jet Propulsion Laboratory, California Institute of Technology,
Pasadena, California 91109, U.S.A.

Abstract. We report on further results of an ongoing programme of radargrammetric experimentation with Space Shuttle Imaging Radar (SIR-B) data. Six stereo models of orbits over Australia were processed in an analytical stereo plotter. Height accuracies were up to ±25 m or 1·8 times the range resolution. This is better than in previous SIR-B stereo work, probably due to better image quality. Some inconsistencies were encountered between look angle geometries and height measurement accuracies. While general observations about earlier SIR-B stereo results were confirmed, inconsistencies with theoretical expectations could not be fully explained.

1. Introduction

Among the land areas covered by overlapping Shuttle Imaging Radar (SIR-B) data, eastern Australia is particularly significant to radargrammetry research. The terrain is topographically accentuated, excellent maps exist and image quality is good. These conditions do not apply in other areas covered by SIR-B images.

The Australian SIR-B coverage is illustrated in figure 1 and consists of three data takes that overlap and form three stereo models (figure 2). Previously analysed data covered Mount Shasta in California (Elachi *et al.* 1986, Ramapriyan *et al.* 1986, Leberl *et al.* 1986 a), Cordon la Graza in Argentina (Leberl *et al.* 1986 b), a flat and rural area in Illinois and the so-called crossover point near José de San Martin, also in Argentina (Domik *et al.*, 1988). Thomas *et al.* (1987) reported on automated Synthetic Aperture Radar (SAR) image mapping using SIR-B coverage of an area in Bangladesh.

The Australian data set covers a large strip of Eastern Australia. The analysis concentrates on the study of coordinate accuracies in two selected areas along the continuously covered radar swath. The current report adds to the body of SIR-B radargrammetry work by analysing six stereo models. The following describes the data, processing methods and results. It will show that coordinate accuracies in height were obtained of about twice the range resolution. This is superior to most previous SIR-B radargrammetry results. Planimetric accuracy was less and amounted to about 5 resolution elements.

Clearly, SIR-B height accuracies do not conform to expectations based solely on geometric analysis. An explanation of the apparent discrepancy between theory and reality is based on thematic differences in overlapping images due to illumination differences. Previous work, e.g. by Kaupp *et al.* (1983) has established a link between

† Present address: Center for Astrophysics and Space Astronomy, University of Colorado at Boulder, Boulder, Colorado 80309-0391, U.S.A.

Figure 1. Location map showing overlapping SIR-B coverage over eastern Australia.

the extent of topographic relief and the stereo perception comfort of an analyst. The relationship with height measurement accuracy is not explored in previous work.

Therefore, the discussion of the SIR-B results must remain speculative until some further controlled experiments, possibly with simulated images, can be performed specifically to address height measurement accuracies and acuity rather than perception comfort.

2. Current data and analysis methods

Table 1 describes the geometry of the Australian SIR-B data sets. An estimate of accuracy can be obtained by theoretical error propagation as discussed in previous work (Leberl *et al.* 1986 a) and is provided in table 2. The intersection angles are detailed in table 3 separately for the three northern and three southern stereo models; they range from 12·9° to 34·5°. Table 2 summarizes the theoretical effect of range errors on the accuracy of object coordinates; it shows that errors should be in the range of 1 to 2 pixels if the theoretical model is applicable, and they should reduce as intersection angles increase.

The radargrammetric analysis is based on Australian maps at scale 1:100 000 with a 20 m contour interval. We estimate that ground control can be extracted from these maps with planimetric errors of ± 50 m and height errors of ± 7 m. The planimetric errors are expected to be affected by map generalization.

Variable numbers of ground control points were extracted from maps and images. Point identification was based on SIR-B image enlargements to the same scale as the map and point selection by superposition of image and map on a light table. Figure 3 presents the control point distribution in one representative stereo model per test area. Nearly 30 control points were identified in each of the test areas covering

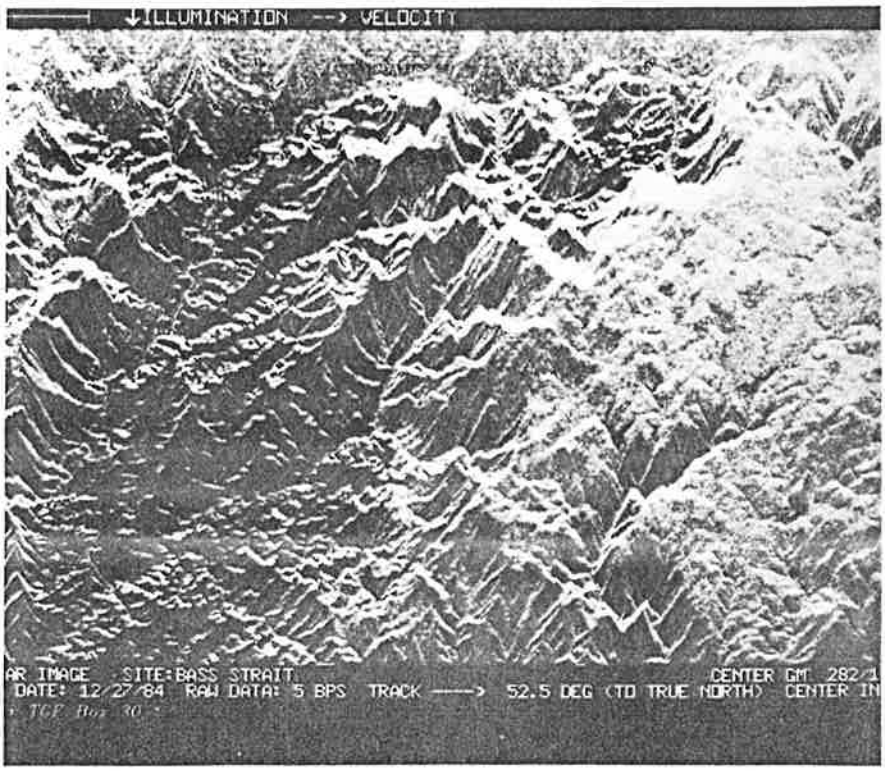

(*a*)

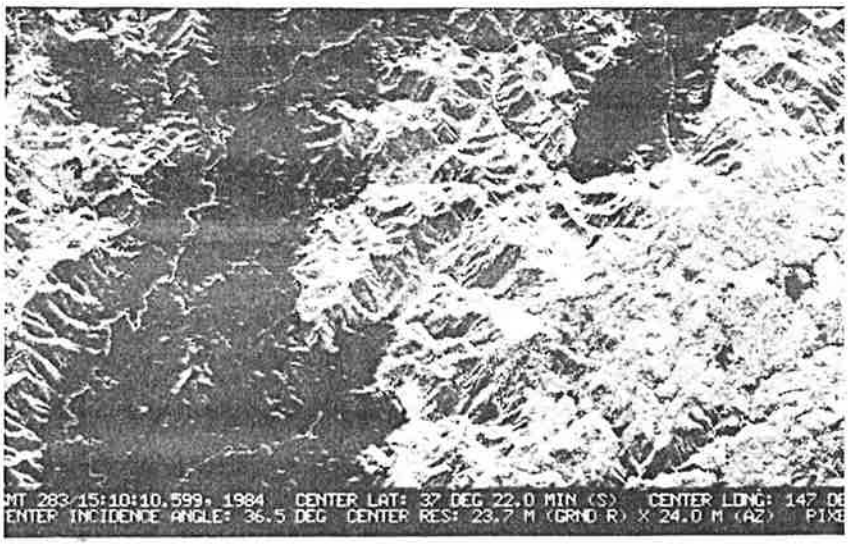

(*b*)

Figure 2. Samples of overlapping SIR-B data takes of eastern Australia. The width of a SIR-B strip is 26 km at steep look angles (cases (*a*) and (*d*)) and 15 km at shallower look angles (cases (*c*) and (*f*)). The annotations on the image edges provide auxiliary information. Near range is up, far range is down. Southern area: SIR-B data takes (*a*) 51.8 (scene 10), (*b*) 67.8 (scene 36) and (*c*) 83.8 (scene 17). Northern area: SIR-B data takes (*d*) 51.8 (scene 15), (*e*) 67.8 (scene 41) and (*f*) SIR-B data take 83.8 (scene 21).

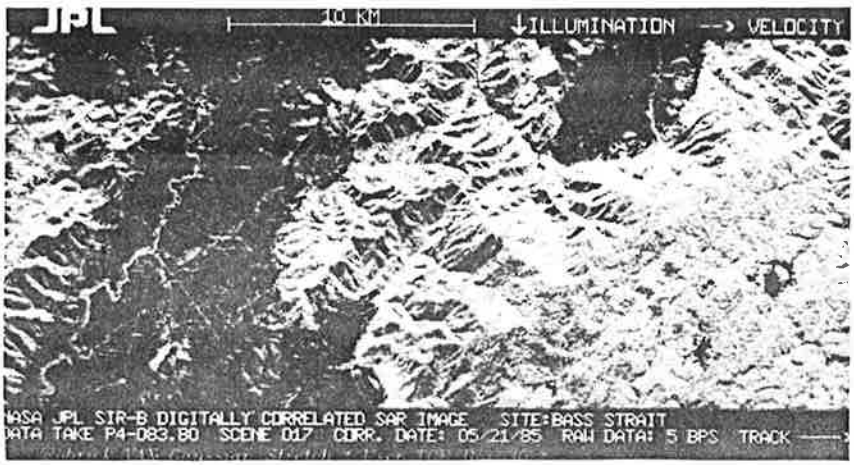

(*c*)

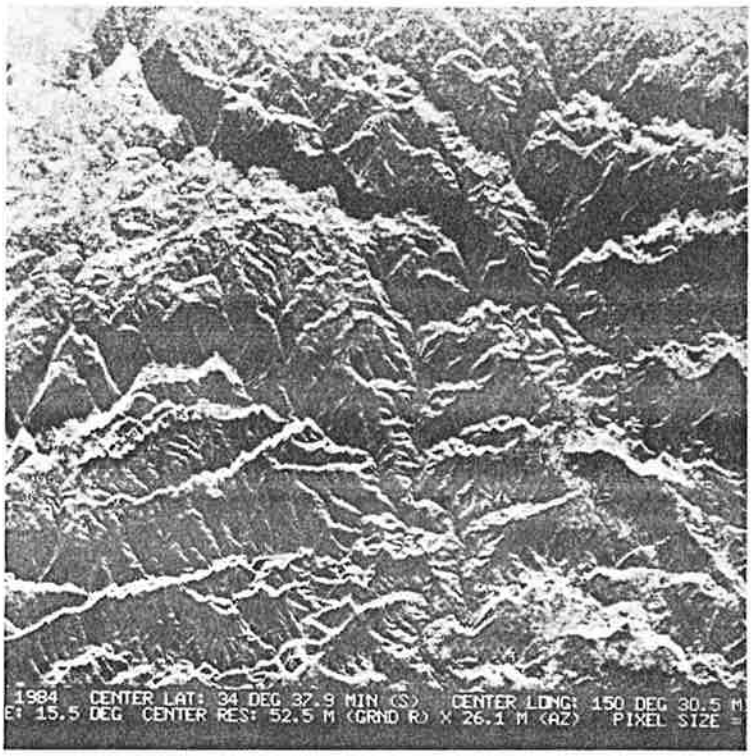

(*d*)

Figure 2 (*continued*).

10 km × 39 km. Points were readily identifiable features that are shown in the map and the images. Not in all stereo models was it feasible to find a large number of control points. Difficulties were particularly great in cases using the steep-looking scenes. Ground control points were measured off the maps and transformed into geographic

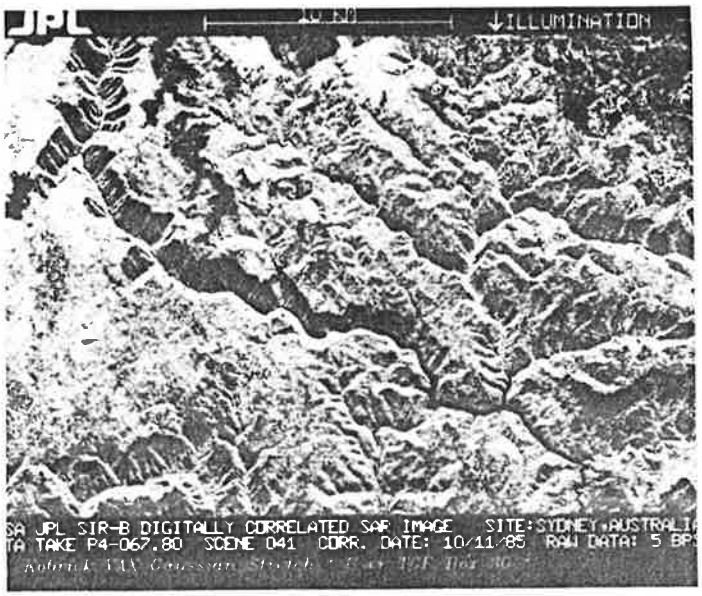

(*e*)

(*f*)

Figure 2 (*continued*).

latitude, longitude and height. In addition, contour lines were manually digitized and used to create a map-derived Digital Elevation Model (DEM).

The radar images, as written onto film, are subject to a stereo radargrammetric process based on the computer program SMART (Raggam *et al.* 1984). The analysis process has been described previously (Leberl *et al.* 1986a). It employs a standard analytical stereo plotter Kern DSR-11. SMART is installed on the host computer of the plotter, a PDP-11. A separate real-time program is loaded into the so-called plate-processor to relate stereo model XYZ coordinates to the image xy- and range/time-coordinates.

The stereo model is first set-up on the instrument so that stereo parallaxes are

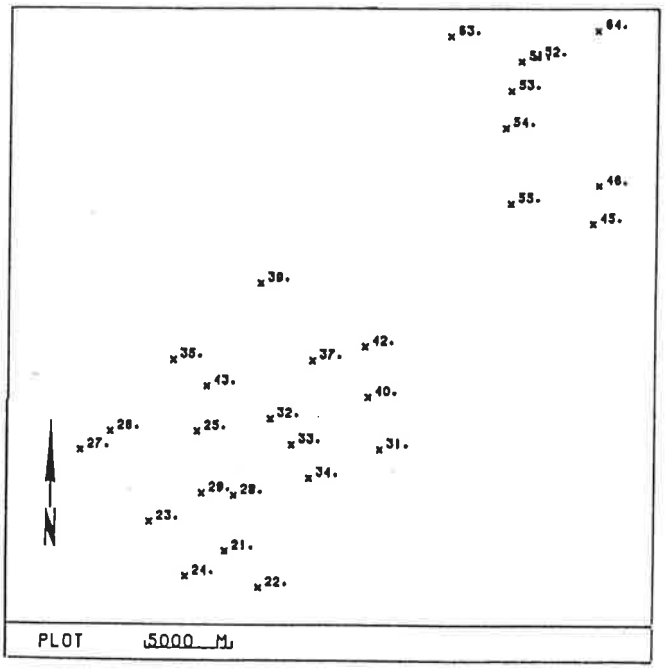

(*a*)

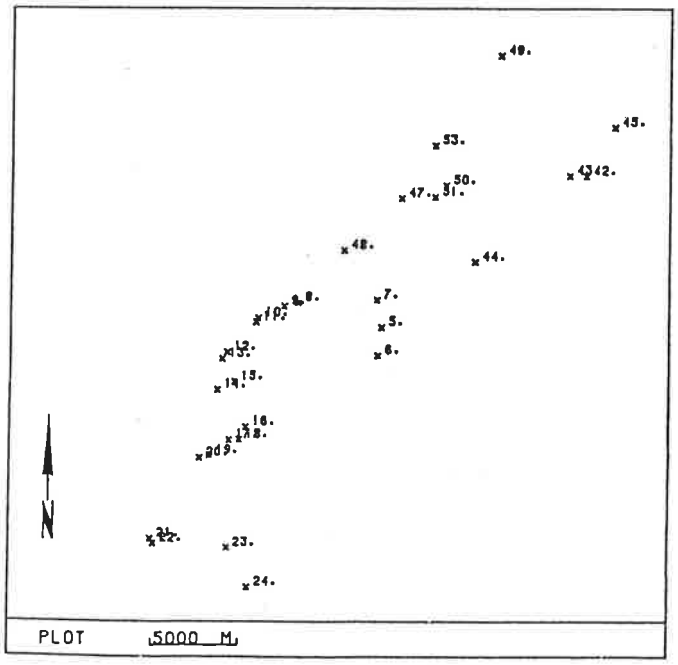

(*b*)

Figure 3. Distribution of ground control points in the two test areas; (*a*) southern area, (*b*) northern area.

Table 1. Australian SIR-B images forming stereo pairs.

Number	Scenes north/south	Data take	Look angle off-nadir (°)	Ground resolution (m^2) range × azimuth
1	15/10	51.8	15	52 × 26
2	41/36	67.8	33	24 × 24
3	21/17	83.8	47	18 × 24

Table 2. Theoretical propagation of range error into height and cross-track coordinates for Australian SIR-B stereo models. Range resolution is 15 m.

Look angle (°)		Intersection angle (°)	Predicted errors	
θ'	θ''		σ_y(m)	σ_h(m)
47	33	14	31	26
33	14	19	28	13
47	14	33	15	10

Table 3. Intersection geometry of Australian SIR-B stereo radar coverage.

Area	Image pair	Intersection angle (°)		Look angle off-nadir centre of overlap (°)
		Near range	Far range	
South/Omeo	17/36	14·2	12·9	47/33
	36/10	20·0	18·8	33/14
	17/10	34·2	31·7	47/14
North/Moss Vale	21/41	13·7	12·5	47/33
	41/15	20·8	19·5	33/14
	21/15	34·6	32·0	47/14

cleared. Then actual terrain elevation data are collected. Most typically this will be in a regular grid pattern for a DEM, or by directly following the contour lines.

3. Results and discussion

3.1. *Coordinate errors*

Table 3 describes the intersection and look angles of the stereo cases. A total of six stereo models were processed; three in the southern and three in the northern area. Tables 4 and 5 summarize the coordinate errors encountered in ground points that were withheld from the computations and tables 6 and 7 show the r.m.s. residuals at the control points. The largest stereo intersection angles produce the highest height accuracy in the southern area. The inverse conclusion does apply to the data from the northern region where the poorest results are from the largest stereo intersection angle.

The order of magnitude of the errors is identical in both areas but the relationship between intersection angle and accuracy is not. One finds the best results to amount to about ±25 m in height; this is better than twice the range resolution (14–15 m).

Table 4. Root mean square discrepancies between radar computed coordinates and those extracted from the map. These points were not used in the model set-up. Southern area.

Model	Total no. of available points	No. of withheld points	Coordinate discrepancies in withheld points (m)			Stereo intersection angle (°)
			X	*Y*	*Z*	
17/36	28	18	93	80	36	14
36/10	29	19	61	77	45	19
17/10	21	11	58	107	22	32

Table 5. Same as table 4. Northern area.

Model	Total no. of available points	No. of withheld points	Coordinate discrepancies in withheld points (m)			Stereo intersection angle (°)
			X	*Y*	*Z*	
41/21	30	20	46	49	25	14
41/15	28	18	112	73	51	19
21/15	10	6	88	83	74	32

Table 6. Root mean square discrepancies between radar and map coordinates at ground control points. Southern area.

Model	No. of control points used	Residuals in control points (m)			Stereo intersection angle (°)
		X	*Y*	*Z*	
17/36	28	69	69	39	14
	15	57	67	36	
	4	116	154	172	
36/10	29	51	78	38	19
	15	32	86	36	
	4	24	39	42	
17/10	21	57	71	28	32
	15	78	76	34	
	4	55	74	31	

However, in the northern area this best accuracy is the result of a small stereo intersection (14°), while in the southern area the best result is from the largest angle (32°). In planimetry the accuracy is poorer and reaches about ± 50 m to ± 80 m per coordinate.

The residual errors in ground control points as presented in tables 6 and 7 are a meaningful measure of point accuracy where point redundancy is high (10 to 30 ground control points). With small numbers of control points (4) the numerical solution for a stereo model set-up can become unstable and residual errors lose significance.

While the absolute accuracy is of interest, it approximates that of some prior SIR-B

Table 7. Same as table 6. Northern area.

Model	No. of control points used	Residuals in control points (m)			Stereo intersection angle (°)
		X	*Y*	*Z*	
41/21	30	41	46	24	14
	15	43	49	27	
	4	29	12	35	
41/15	28	76	65	27	19
	10	118	89	72	
	4	138	113	100	
21/15	10	84	70	66	32
	7	97	72	49	
	4	98	45	96	

studies. What is surprising however, is the discrepancy between the two areas. We discuss this finding in § 3.4.

3.2. *Stereo acuity*

A separate experiment served to quantify the definition of the ground surface. Several operators independently set the stereo measuring mark on the ground surface in a small horizontal area to define the repeatability of a surface height measurement. Repeating the measurement of height several times (five and six times per operator) at different but closely-spaced locations in a flat area produces a measure of surface definition; one obtains an r.m.s. spread of the height measurement. In the southern area (table 8) the height sensitivity (stereo acuity) improves with larger intersection angles from ± 14 m to ± 8 m; in the northern area (table 9) it deteriorates from ± 10 m to ± 15 m as the intersection angles increase. Again, this confirms the surprising result already obtained from the control point measurements.

Table 8. Stereo acuity expressed as r.m.s. error of height in metres measured by repeatably (twelve times) setting the measuring mark on the ground in a flat area by two operators. Southern area.

Model	R.m.s. (m)	Stereo intersection angle (°)
17/36	14	14
36/10	8	19
17/10	8	32

Table 9. Same as table 8 using ten observations by two operators. Northern area.

Model	R.m.s. (m)	Stereo intersection angle (°)
41/21	10	14
41/15	12	19
21/15	15	32

3.3. *Digital elevation models*

A final result exists in the form of a DEM. This was created from one radar stereo model and one map. Processing of the elevation data was based on manually digitized map contour lines, and on near-regular grid measurements from the radar stereo model. Presentation of the DEM data is in the form of a shaded relief perspective (figures 4, 5, and 6). The r.m.s. difference between height estimates in figures 4 and 5 is given by the r.m.s. value of the function in figure 6 and is equal to ± 24 m.

3.4. *Discussion of accuracies*

The type of presentation in figures 4–6 and tables 4–7 is commonly used to describe mensuration results and accuracies in photogrammetry. The accuracy results themselves however, require further scrutiny. Figures 7 and 8 show height error vectors in a selected stereo model from each area. The two areas are clearly different in spite of the fact that points are equally well distributed; the northern area is somewhat narrower. The error vectors represent only one of three computation cases of each area, namely the one with 28 ground control points in the southern area and 29 points in the northern one. It is evident that the errors are somewhat systematic; adjacent points will have similar error vectors. However, the sign and magnitude of errors change often. The computational models for satellite SAR stereo work do not provide for high spatial frequency errors. Neither has there been any suggestion that higher frequency errors should exist. First, satellite orbits are stable and unperturbed over periods of a few seconds and secondly, radar imaging should not introduce geometric image deformations, certainly not at high spatial frequencies.

The numerical work is surprising due to the opposing trends in the two test areas; in the northern case height accuracies seem to deteriorate as intersection angles increase,

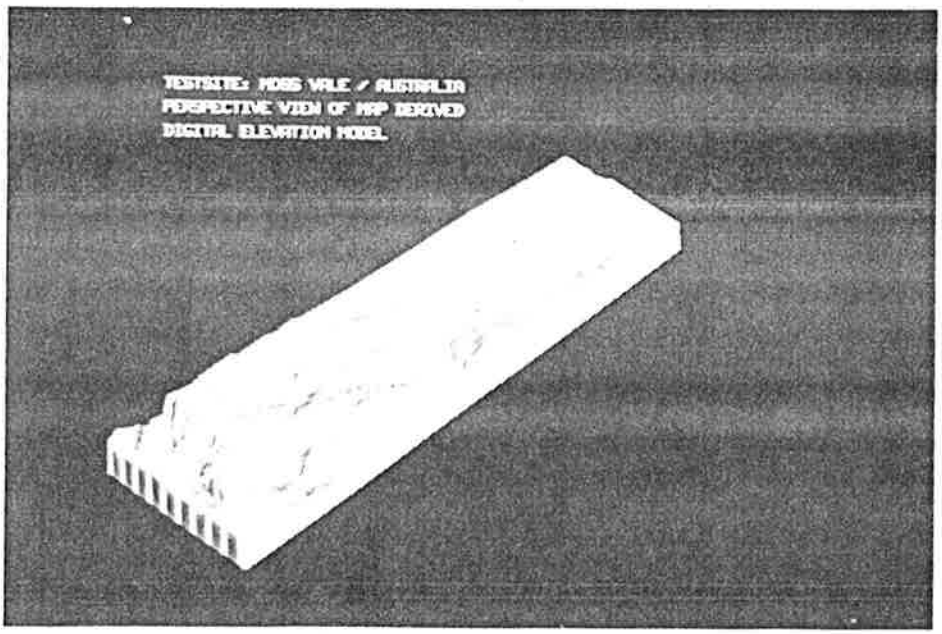

Figure 4. Perspective view of the map-derived DEM, consisting of about 60 × 240 points.

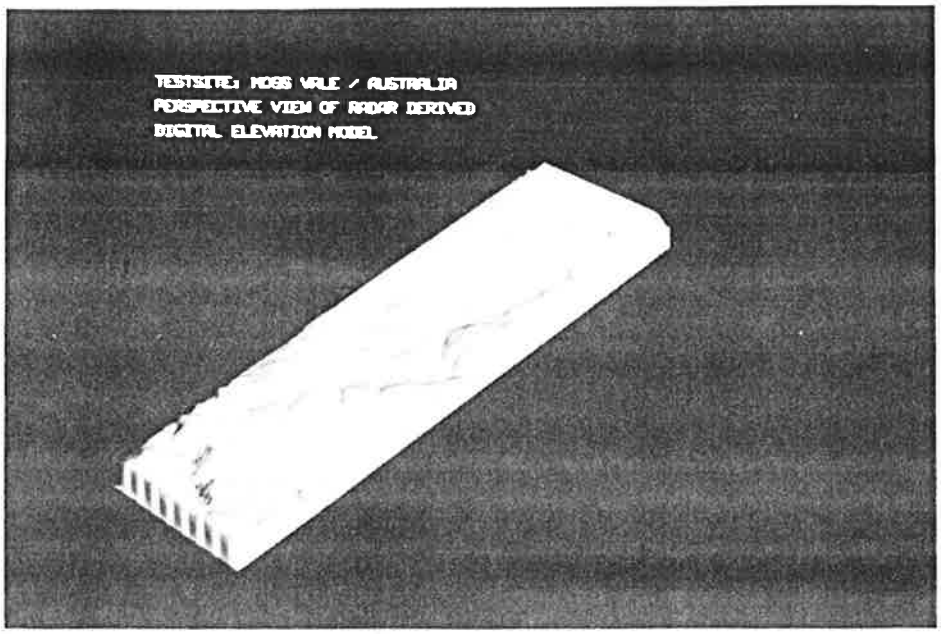

Figure 5. Same as figure 4 but radar-derived.

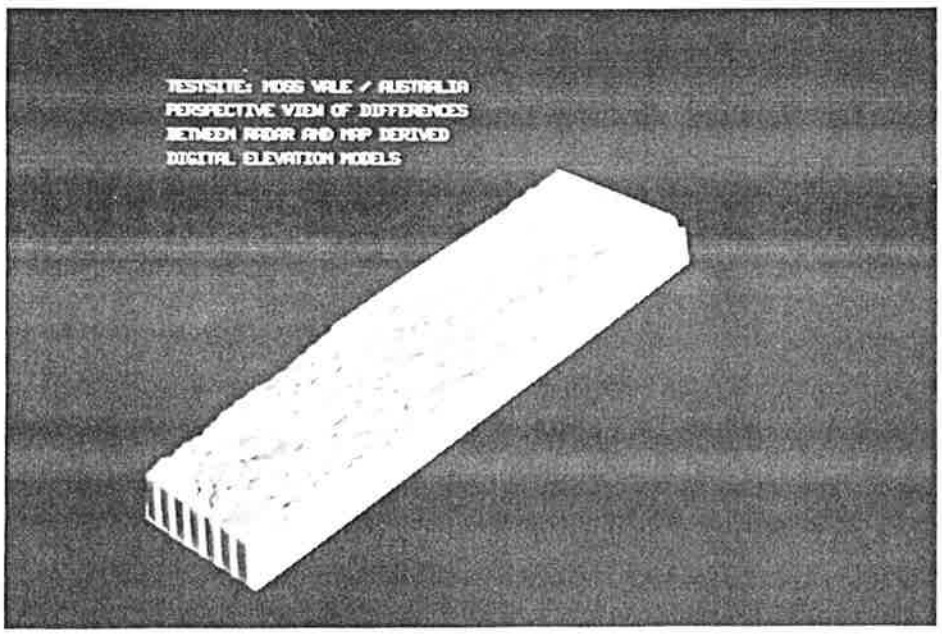

Figure 6. Perspective view of the difference DEM, consisting of 60×240 points. R.m.s. difference is ± 24 m.

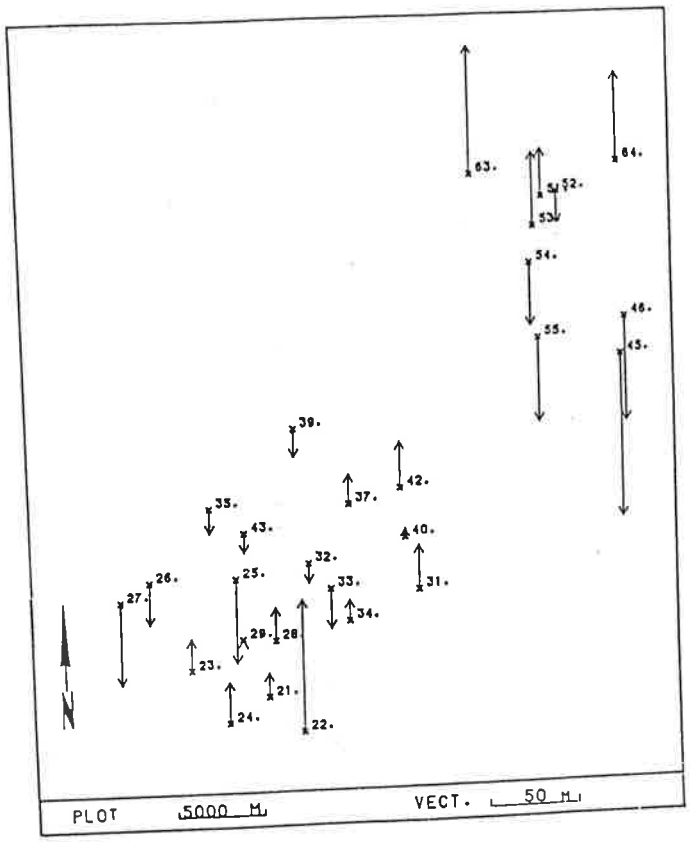

Figure 7. Height residuals in stereo model 17/36 (southern area).

in the southern area they improve. This inconsistency can only be explained with reference to the images themselves. Figures 2 (*b*) and (*d*) show the steep look angle images and their differences from the shallower look angle images. One must anticipate difficulties of stereo fusion when employing pairs of images with large look angle differences, as discussed by Kaupp *et al.* (1983). Simulations by Kaupp *et al.* (1983) have shown an increased viewing comfort at smaller intersection angles if terrain relief increased. However, quantitatively, Kaupp *et al.* (1983) discuss intersection angles at 30°–40°. This is rather large compared to the 13°–32° in the Australian SIR-B base. In addition, it is unclear how perception comfort translates into stereo acuity and height accuracy.

We have found in several instances that increasing the geometric strength of larger stereo intersection angles does not necessarily translate into better height accuracies. The larger intersection disparity will normally cause larger thematic differences and therefore reduce the quality of the image match (Leberl *et al.* 1986 b). It appears that the thematic differences due to look angle disparities are more distinct in the northern area than in the south where the area is smoother and less topographic relief exists. The exploitation of the increase in geometric strength may therefore be a function of the type of terrain, as has been indicated in earlier work (Leberl 1979, Kaupp *et al.* 1983).

Unfortunately, to blame the inconsistencies in height accuracies solely on relative

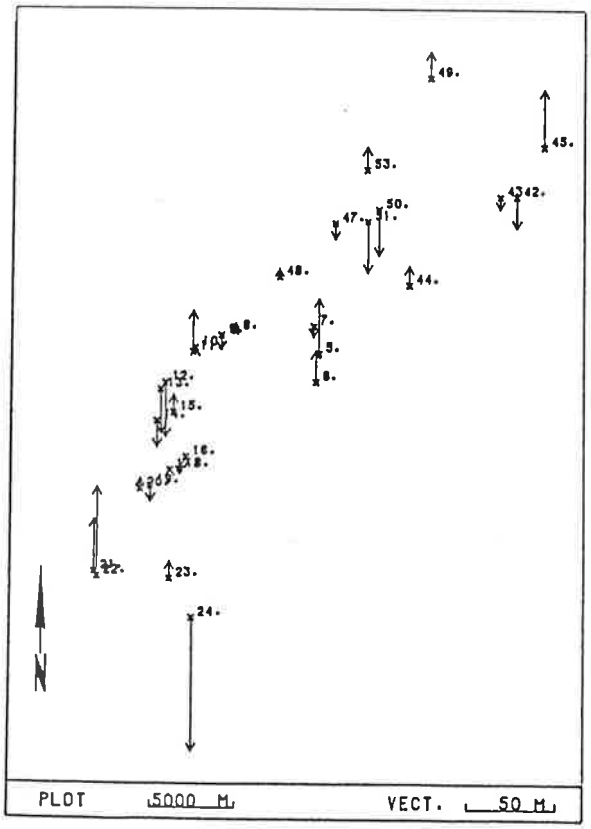

Figure 8. Height residuals in stereo model 41/21 (northern area).

topographic relief may not be entirely correct; the acuity tests of tables 8 and 9 were done in flat terrain segments of both areas. Still the inconsistencies occur. One may have to look for signal-to-noise ratios or other factors that may cause stereo acuities to decrease.

While there is inconsistency in the height (and along-track) coordinates, there is consistency in decreasing the cross-track accuracy as intersection angles increase. We can argue that planimetric accuracy is largely dependent on the identifiability of ground control points. Since these points are taken from a 1:100 000 scale map we may have to expect errors of $\pm 0{\cdot}5$ mm in the image or ± 50 m on the ground. This seems indeed to be the lower bound on the current planimetric SIR-B accuracy values. However, increasing SAR look angle disparities should theoretically improve the cross-track (y) coordinate accuracy (see table 2) when in fact it does not (see tables 4 and 5). As we found in earlier anlyses, it seems that accuracies are affected by thematic differences as a result of relative terrain relief, and possibly by other factors such as noise levels, and do not conform to the expectations based on intersection geometry.

4. Conclusions

The analysis of SIR-B stereo radar data has covered areas in the U.S.A., Argentina and now has dealt with areas in Australia. This has produced excellent height

accuracies of up to 1·8 times the range resolution. Planimetric accuracy may be limited by errors of map-derived ground control to about ±50 m.

The data set from Australia has highlighted the major problem of stereo-radargrammetry; improved geometric strength of an intersection configuration is counteracted by increased thematic differences. In certain cases the coordinate accuracy does not improve when intersection angles increase. This fact was first encountered in a set of four SIR-B images in Argentina and three images of Mount Shasta (Leberl *et al.* 1986 a, Leberl *et al.* 1986 b). In the current data set two opposing trends are observed, deterioration of accuracy with increase of intersection angles from 14° to 33° and improvement of accuracy in another case when intersection angles change from 15° to 32°.

SAR image simulations by Kaupp *et al.* (1983) and others have been used in the past to address the stereo perception comfort, not height accuracy. The simulations indicated a decrease in perception comfort if terrain is more accentuated and mountainous. However, this observation by itself does not explain the results in stereo acuity within flat terrain segments of the Australian SIR-B data.

These results point to a need to quantify the interdependence between look angles off-nadir, terrain type and positioning accuracy. We see the need to design a controlled experiment with simulated radar images, and to quantify the stereo observation abilities of a human operator by an image correlation algorithm. While comfort of stereo perception is of great interest to the analysing photo-interpreter, it is not a measure of height accuracy.

Additional SIR-B stereo imagery exists of Bangladesh and Nevada but only in the form of single image pairs. The completion of the SIR-B stereo mapping experiment requires an accuracy evaluation for these two areas as well; however, we anticipate confirmation of earlier conclusions on the paradigm between geometric strength and thematic disparity.

Acknowledgments

We are grateful for the help of Dr John Trinder who provided maps of the study area. Ms Annie Holmes of JPL arranged for photo work. Diana Allen and Jeff Coe did the stereo observations, Erwin Kienegger the perspective views of the surface data. The contributions by VEXCEL to the work for this paper were performed under Contract No. 757549, Subtask 'Australia', for the California Institute of Technology Jet Propulsion Laboratory.

References

Domik, G., Leberl, F., and Cimino, J., 1988, Dependence of image grey values on topography in SIR-B images. *International Journal of Remote Sensing*, **9**, 1013–1022.

Domik, G., Leberl, F., and Cimino, J., 1986, Multiple incidence angle SIR-B experiment over Argentina: Generation of secondary image products. *I.E.E.E. Transactions on Geoscience and Remote Sensing*, **24**, 492–497.

Elachi, C., Cimino, J., and Settle, M., 1986, Overview of the Shuttle Imaging Radar-B preliminary scientific results. *Science, New York*, **232**, 1477–1576.

Kaupp, V. H., Bridges, L. C., Pisaruck, M. A., McDonald, N. C., and Waite, W. P., 1983, Simulation of spaceborne stereo SAR-imagery: Experimental results. *I.E.E.E. Transactions on Geoscience and Remote Sensing*, **21**, 400–405.

Leberl, F., 1979, Accuracy analysis of stereo side-looking radar. *Photogrammetric Engineering and Remote Sensing*, **45**, 1083–1096.

Leberl, F., Raggam, J., Domik, G., and Kobrick, M., 1986 a, Radar stereomapping techniques and application to SIR-B images of Mt. Shasta. *I.E.E.E. Transactions on Geoscience and Remote Sensing*, **24**, 473–481.